Dispersion of exciton-polariton based on ZnO/MgZnO quantum wells at room temperature*

Huying Zheng(郑湖颖)[1], Zhiyang Chen(陈智阳)[1], Hai Zhu(朱海)[1,†], Ziying Tang(汤梓荧)[1], Yaqi Wang(王亚琪)[1], Haiyuan Wei(韦海园)[1], and Chongxin Shan(单崇新)[2]

[1] *State Key Laboratory of Optoelectronic Materials and Technologies, School of Physics, Sun Yat-Sen University, Guangzhou* 510275, *China*
[2] *Key Laboratory of Materials Physics of Ministry of Education, School of Physics and Microelectronics, Zhengzhou University, Zhengzhou* 450052, *China*

(Received 29 April 2020; revised manuscript received 4 June 2020; accepted manuscript online 5 June 2020)

We report observation of dispersion for coupled exciton-polariton in a plate microcavity combining with ZnO/MgZnO multi-quantum well (QW) at room temperature. Benefited from the large exciton binding energy and giant oscillator strength, the room-temperature Rabi splitting energy can be enhanced to be as large as 60 meV. The results of excitonic polariton dispersion can be well described using the coupling wave model. It is demonstrated that mode modification between polariton branches allowing, just by controlling the pumping location, to tune the photonic fraction in the different detuning can be investigated comprehensively. Our results present a direct observation of the exciton-polariton dispersions based on two-dimensional oxide semiconductor quantum wells, thus provide a feasible road for coupling of exciton with photon and pave the way for realizing novel polariton-type optoelectronic devices.

Keywords: quantum wells, exciton, polariton, microcavity

PACS: 73.21.Fg, 71.35.–y, 42.55.Sa, 71.36.+c **DOI:** 10.1088/1674-1056/ab99b3

1. Introduction

Exciton polaritons are the quasiparticles resulted from the coupling between photons confined in a microcavity and excitons. A polariton laser is not based on the stimulated emission of photons but on the coherence condensation process of exciton polaritons in the lowest energy state.[1,2] Therefore, the lasing threshold is expected to be very low. In the past ten years, the properties of polariton have been very extensively studied, and a set of striking phenomena have also been demonstrated. Such as parametric optical scattering,[3] spontaneous Bose–Einstein condensation (BEC) at high temperature,[4,5] superfluidity,[6] and even quantized vortex.[7] In principle, these unique properties serve as a basis for development of series novelty optoelectronic devices: polariton lasers,[8,9] polariton switches.[9] A key principle advantage of exciton polaritons is the achievement of the strong coupling regime (SCR) at room temperature (RT) and realization of the electrical injected polariton devices. Although the BEC lasing has been observed in organic materials,[10,11] the electrical injection is still its bottleneck in the operation. Therefore special attention and huge technological efforts have turned to wide-band gap semiconductors, such as GaN and ZnO. The advantage of using such semiconductors with a large exciton binding energy and oscillator strength is that a polariton laser based on such a material would be able to operate at RT, which is an absolute requirement for a commercial device.

For ZnO, both exciton oscillator strength and binding energies (60 meV) are much larger than those for nitrides.[12–15] As a result, the energy splitting between the polariton eigenmodes can reach 100–200 meV, a record for inorganic structures. Up to date, some self-constructed cavities based on ZnO nanosturcture, such as microwires, have demonstrated the SCR at RT.[16–18] It has been anticipated that the two-dimensional (2D) ZnO quantum structure will be an optimum choice for polariton devices in the blue-UV range.[19–21] However, the vertical cavity structure with bottom dielectric distributed Bragg reflector (DBR) deteriorates the crystalline quality dramatically and results to huge spatial inhomogeneous broadening. In order to realize the ZnO polariton in SCR at RT, the broadening effect resulted from interface disorder scattering in 2D QW must be suppressed.

In this work, we investigate microcavity polariton that exhibits the excellent exciton properties of ZnO/MgZnO QWs grown on sapphire substrates enabled by single top dielectric DBRs. The complex buffer layer for QW deposition is introduced, thereby the crystalline quality of active layer is enhanced. It is demonstrated that the excellent crystalline quality of the QWs in this structure can be used to explore the dispersion properties of polariton at RT. The tapered cavities also allow the observation of polariton dispersion behavior at different detunings.

*Project supported by the National Natural Science Foundation of China (Grant Nos. 11974433, 91833301, and 11974122), the Guangdong Natural Science Fund for Distinguished Young Scholars, China (Grant No. 2016A030306044), and the Science and Technology Program of Guangzhou, China (Grant No. 201707020014).

†Corresponding author. E-mail: zhuhai5@mail.sysu.edu.cn

2. Discussion

The microcavity samples used in our experiment, consisting four-period ZnO/$Mg_{0.15}Zn_{0.75}O$ QWs, were grown by MBE on sapphire substrates. Here the bottom MgZnO spacer layer was tapered along one direction of the sample so that the resonant photon frequency of the cavity varied with sample position. Then 20 pairs Zr_2O_3/SiO_2 dielectric top DBR (reflectivity of 99.5%) were deposited on the sample, hence the thickness of cavity was gradient whose value depended on the exact location of the sample as shown by the schematic diagram of the device (Fig. 1(a)). Considering the total reflection mirror of top DBR, the output of polariton emission signal was collected from the bottom double-polish Al_2O_3 substrate. Then, the light was analyzed by a $4f$ angle-resolved PL system. Such a thickness gradient cavity allows for a tuning of the energies of the cavity modes and the resulting dispersion of polariton branch.

In contrast to the bare ZnO film, the PL spectrum of QW sample at RT displays a dominant peak from the well region without the defect related emitting band (Fig. 1(b)). Meanwhile, the emission shoulder at the higher energy that resulted from the barrier layer can also be seen obviously. Furthermore, low-temperature (77 K) PL spectrum of QW is present (Fig. 1(c)), which shows the precise free-exciton (FX) peak and three phonon replica from the QW. The energy of FX peak increases because of spatial confinement for exciton state in the 2D well structure. The appearance of three-order LO-phonon replicas confirms the excellent optical properties of QWs. Benefited from high exciton binding energy (E_b), the excitons will be interacted strongly with confined photons in cavity. On the other hand, the larger oscillator strength can override the leakage loss of photon, it is anticipated that the strong coupling with larger Rabi splitting will be realized in the plate microcavity.

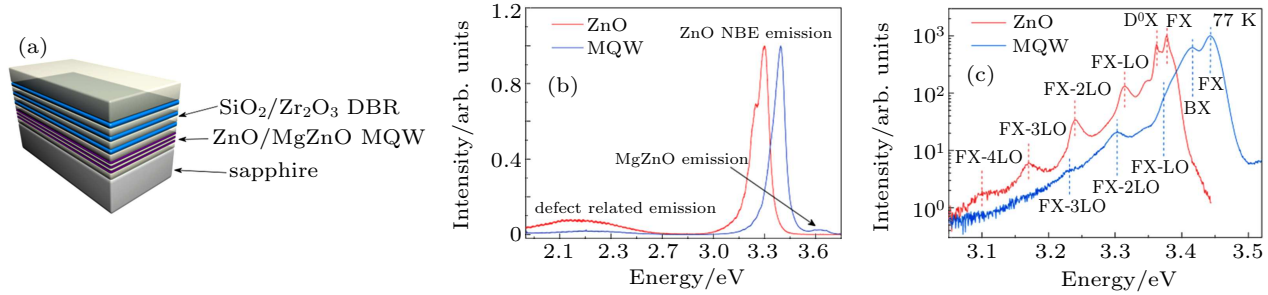

Fig. 1. The microcavity structure and optical property of ZnO QWs. (a) Schematic diagram for vertical cavity structure of ZnO QWs. The four-period ZnO QWs are grown on the sapphire substrate and then top Zr_2O_3/SiO_2 DBR was deposited on it. (b) PL spectrum of bare ZnO films and ZnO-based QWs at RT. Due to the spatial potential confinement, the radiation energy of exciton in QWs is larger than that of FX in the bare film. (c) Low-temperature (77 K) PL spectrum of QWs, which shows three phonon replica and free exciton.

The typical angle-resolved polariton dispersion characteristics of our sample under nonresonance excitation were investigated (Fig. 2). Four emission bands can be observed, generally the obtained emission of polariton is from the lower polariton (LP) branch and the upper polariton (UP) is absent (left panel). One reasonable explanation of the absence of the UP branch is that the interaction between polariton and phonon via the exciton component is very strong at RT. Therefore, the polaritons in the UP branch are quickly decayed to the LP, hence the emission from the UP branch is strongly suppressed. It is remarkable that the dispersion of polariton based on ZnO QWs can be clearly resolved even upon RT. The exciton-like dispersion is spectrally narrow, being very weakly affected by the photonic inhomogeneous broadening induced by the thickness gradient. On the other hand, the more photonic-like dispersion exhibits a large inhomogeneous broadening, with several neighboring modes visible.

By taking the cavity resonance condition and the polariton dispersion into account, one can get an exact expression for the polariton dispersion in the planar cavity as[22]

$$E_{\mathrm{LP,UP}}(k_{\parallel}) = \frac{1}{2}\left[E_{\mathrm{ph}}(k_{\parallel}) + E_{\mathrm{ex}}(k_{\parallel})\right] \pm \frac{1}{2}\sqrt{\left[E_{\mathrm{ph}}(k_{\parallel}) - E_{\mathrm{ex}}(k_{\parallel})\right]^2 + 4g_0^2}, \quad (1)$$

where g_0 is the normal mode splitting, and the damping term is neglected. We carried out a computational analysis using Eq. (1), and give the calculated results (solid curves in the right panel of Fig. 2). As illustrated, the theoretical calculations for the dispersion properties of LP branches give an accurate fit to the experiments, and the Rabi splitting is deduced to be about 60 meV from the calculation theoretically.

It is noted that the dominant emission spot located at high $k_{\parallel}$ is bright than that at low energy state ($k_{\parallel} = 0$), here the intensities of spectra have been normalized. This phenomenon can be attributed to phonon bottleneck effect in the low-dimensional quantum structure. Although the relaxation of LP is hindered due to the pronounced photon-like character of LP, this bottleneck can be overcome directly by increasing the temperature to favor polariton-phonon interactions or polariton-polariton scattering in the medium.[23]

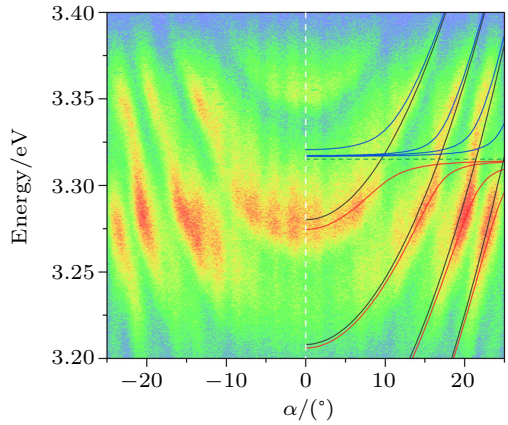

Fig. 2. Angle-resolved PL spectra of ZnO/MgZnO QWs (left) and theoretical fitting curve (right). The dispersion exhibits a large inhomogeneous broadening with the Rabi splitting of about 60 meV that deduced from fitting. The solid lines represent the coupled UP (blue line) and LP branch (red line), respectively. Meanwhile, the black solid and the horizontal dashed lines point the exciton energies and the bare uncoupled cavity mode dispersion for reference.

To illustrate the exciton-polariton comprehensively, the detailed numerical calculation results about dispersion with damping term are given in Fig. 3. In the simulation, we consider the decay of the exciton and photon in the cavity with the Lorentz model. The measurement data (left panel) is surprisingly in agreement with the results of rigorous coupled-wave analysis (right panel). Color maps of the measured PL spectra at RT are normalized for the purpose of highlighting the variation of polariton dispersion curves. It is given that three polariton modes are accompanied with very different excitonic contents. The distribution of polariton particles in LP branches will reach the bottom of LP through thermodynamically process.

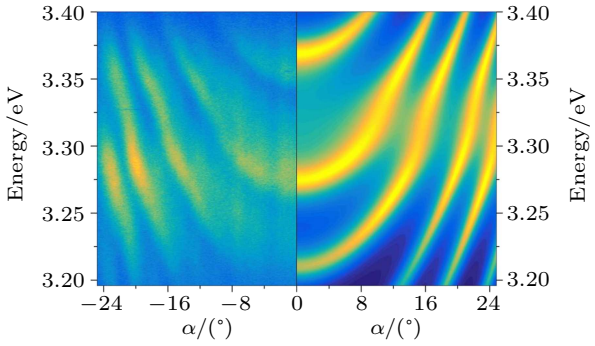

Fig. 3. Angle-resolved dispersion of exciton-polariton and the simulation results. Color maps of the measured PL spectra are normalized for the purpose of highlighting the variation of polariton dispersion curves (left panel). The measurement is in agreement with the numerically calculated results of rigorous coupled-wave analysis (right panel).

Furthermore, for a given exciton-photon detuning, the polariton dispersion pattern versus externally pumping power is investigated (Fig. 4). When the pump intensity is lower, the distributions of polaritons in k-space in LP and UP branches are equal (Fig. 4(a)). Meanwhile, the color maps of dispersions indicate that the exciton fraction is about 11% with the detuning of $\delta = -110$ meV. With increasing excitation power, the LP exhibits an intense intensity than UP accounting for the relaxation between two branches (Figs. 4(b) and 4(c)). It is noted that the relaxation process of polariton in LP branch appears well and is wide in k-space due to its interaction with the excitonic reservoir. With further increase of the pump intensity, the enhanced exciton-exciton scattering processes will stimulate the faster relaxation of polariton to reach the bottom of LP branch (Fig. 4(d)).

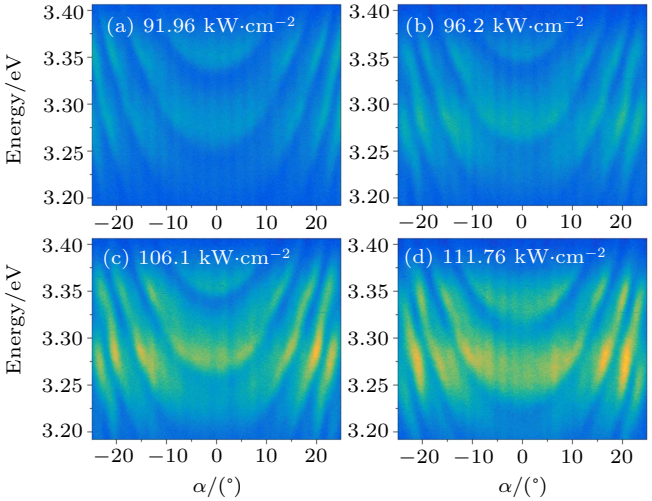

Fig. 4. Analysis of the LP characteristics of polaritons as a function of pumping intensity. (a) As the pump intensity is very lower, the polaritons distributed in k-space are very few. (b), (c) With increasing excitation power, the emission pattern of LP is enhanced dramatically for the case of 96 kW·cm^{-2} and 106 kW·cm^{-2}. (d) At high pumping power (111 kW·cm^{-2}), the LP branch exhibits a magnitude population occupancy that accounts for the relaxation between LP and UP.

By scanning the excitation spot along the tapered cavity, the dispersions of exciton-polariton can be manipulated (Fig. 5). Experimentally, the PL signal was collected from normal direction of the sample at different positions. The height change of expitaxy layer results in the variation of cavity thickness, which corresponds to the different detunings between exciton and photon. A simulated features based on the numerical solution give further insight into the behavior of polariton distribution in these cavities. The detuning ranges from −22 meV to 4.5 meV, meanwhile the Rabi splitting ranges from 50 meV to 80 meV, extracted from the theoretical fitting of the dispersions. The k-space distribution of polariton in the LP for $\delta = -22$ meV shows a wide homogeneous due to the interaction between polaritons (Fig. 5(a)). With the detuning changing, a remarkable variation can be achieved in polariton distribution, where bottleneck in LP branch will be eliminated efficiently (Fig. 5(b)).

At intermediate detuning ($\delta = -8$ meV), the distribution merges to form a single LP branch (Fig. 5(c)). Subject to the trade-off between the thermodynamic (negative detuning) and kinetic (positive detuning) requirements, polaritons

will select the optimal branch to condense.[23] Remarkable, just a single UP branch can be seen clearly as the detuning ($\delta = 4.5$ meV) going to less positive (Fig. 5(d)), which is continuously observed from the same mode. As the hybrid state becomes too much photonic-like with higher excitation power, the system is closed to conventional stimulated emission. In contrast with the result in GaN based cavities[25] under the same temperature condition, the optimal detuning of our QW structure is positive, which is consistent with the result theoretically expected.[26] This behavior may be due to the large Rabi splitting value and a very deep energy minimum at the bottom of the LP branch. The intrinsic scheme about our achievement will require further investigation on the polariton–polariton interaction in ZnO-based QW microcavities.

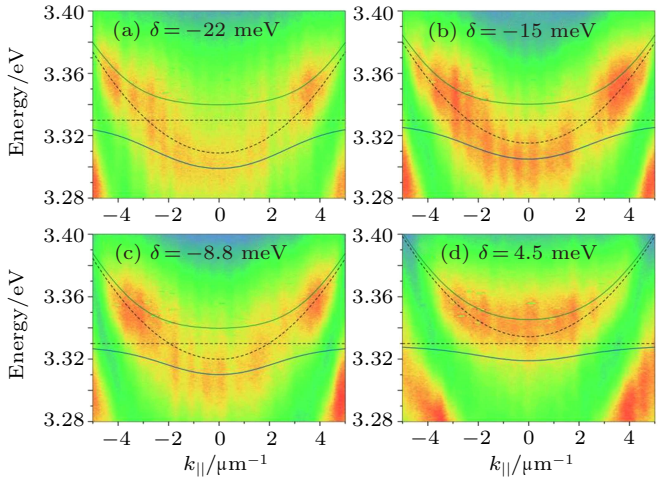

Fig. 5. Color maps of angle-resolved PL spectra of ZnO QWs at different positions with different detunings. (a) For the large negative detune of −22 meV, the polariton emission is very weak, which can be attributed to the low coupling efficiency between cavity-photon and exciton. The solid (dashed) line shows the calculated dispersion of polariton (bare cavity modes and exciton state). (b) and (c) Images of polariton taken in the cases of $\delta = -15$ meV and −8.8 meV, respectively. (d) The emission pattern of polariton just shows a UP branch solely, as the detuning is about 4.5 meV.

3. Conclusion

In summary, we have demonstrated the 2D ZnO-based QWs combining high exciton binding energy coupling with photons in a dielectric plate microcavity, which allows us to explore polariton dispersion at RT and to tune the detuning between photons and excitons. Beyond the technological interest, these new hybrid dielectric DBR cavity structures open a very interesting perspective to perform lasing experiments and to study the temperature and exciton fraction dependences of the BEC behavior in polariton.

4. Structure fabrication and characterization

The ZnO/MgZnO QW samples under investigation were grown on (001) sapphire substrates by a plasma-assisted molecular beam epitaxy system. Elemental Mg (6N) and Zn (6N) were supplied by solid source effusions cells. Oxygen was cracked by a radio-frequency (RF) plasma generator (Oxford Applied Research HD 25) for O source. Before growth, the substrate was annealed at 750 ℃ under vacuum $\sim 10^{-9}$ Torr for 15 min, and subsequently exposed in oxygen plasma to make the surface of (0001) Al_2O_3 O-terminated. A designed four-step buffer layers[27] were deposited in sequence for reducing the mismatch between the epitaxial films and the substrate. For the QW, four periodic intrinsic ZnO/$Mg_{0.15}Zn_{0.75}O$ (6 nm/12 nm) layers were deposited at 600 ℃ after the buffer layers growth, then 60-nm-thick MgZnO was used to form a cap layer.

The whole growth process was monitored by an *in situ* reflection high energy electron diffraction device in MBE. In the experiment, the PL spectra of the QW sample were measured with a He-Cd laser (325 nm) through a μ-PL system. Low temperature (77 K) PL was carried out using an He-Cd laser with the samples in an open-cycle liquid N_2 cryostat. The dispersion features from the device were excited by nonresonant continuous waves and collected by an angle-resolved μ-PL system, then was analyzed by a spectrometer equipped with a silicon charge-coupled device.

FDTD simulations were carried out to provide numerical calculation results. The excited source in QWs was selected as dipole, and the dispersion characteristics of polaritons were calculated using the coupling wave equation.

References

[1] Deng H, Weihs G, Santori C, Bloch J and Yamamoto Y 2002 *Science* **298** 199
[2] Kasprzak J, Richard M, Kundermann S, Baas A, Jeambrun P, Keeling J M J, Marchetti F M, Szymanska M H, Andre R, Staehli J L, Savona V, Littlewood P B, Deveaud B and Dang L S 2006 *Nature* **443** 409
[3] Romanelli M, Leyder C, Karr J P, Giacobino E and Bramati A 2007 *Phys. Rev. Lett.* **98** 106401
[4] Byrnes T, Kim N Y and Yamamoto Y 2014 *Nat. Phys.* **10** 803
[5] Sanvitto D and Kena-Cohen S 2016 *Nat. Mater.* **15** 1061
[6] Lerario G, Fieramosca A, Barachati F, Ballarini D, Daskalakis K S, Dominici L, De Giorgi M, Maier S A, Gigli G, Kena-Cohen S and Sanvitto D 2017 *Nat. Phys.* **13** 837
[7] Lagoudakis K G, Wouters M, Richard M, Baas A, Carusotto I, Andre R, Dang L and Deveaud-Pledran B 2008 *Nat. Phys.* **4** 706
[8] Christopoulos S, von Hogersthal G B H, Grundy A J D, Lagoudakis P G, Kavokin A V, Baumberg J J, Christmann G, Butte R, Feltin E, Carlin J F and Grandjean N 2007 *Phys. Rev. Lett.* **98** 126405
[9] Kang J W, Song B Y, Liu W J, Park S J, Agarwal R and Cho C H 2019 *Sci. Adv.* **5** eaau9338
[10] Ballarini D, De Giorgi M, Cancellieri E, Houdre R, Giacobino E, Cingolani R, Bramati A, Gigli G and Sanvitto D 2013 *Nat. Commun.* **4** 1778
[11] Kéna-Cohen S and Forrest S R 2010 *Nat. Photon.* **4** 371
[12] Daskalakis K S, Maier S A, Murray R and Kéna-Cohen S 2014 *Nat. Mater.* **13** 271
[13] Zhao F Q, Zhang M and Bai J H 2015 *Chin. Phys. B* **24** 097105
[14] Chen A Q, Zhu H, Wu Y Y, Yang D C, Li J Y, Yu S F, Chen Z Y, Ren Y H, Gui X C, Wang S P and Tang Z K 2018 *Adv. Opt. Mater.* **6** 1800407
[15] Liang Y C, Liu K K, Lu Y J, Zhao Q and Shan C X 2018 *Chin. Phys. B* **27** 078102

[16] Lu Y J, Shi Z F, Shan C X and Shen D Z 2017 *Chin. Phys. B* **26** 047703
[17] Sun L X, Chen Z H, Ren Q J, Yu K, Bai L H, Zhou W, Xiong H, Zhu Z Q and Shen X C 2008 *Phys. Rev. Lett.* **100** 156403
[18] Duan Q, Xu D, Liu W, Lu J, Zhang L, Wang J, Wang Y, Gu J, Hu T, Xie W, Shen X and Chen Z 2013 *Appl. Phys. Lett.* **103** 022103
[19] Zhang S F, Wei X, Dong H, Sun L, Ling Y, Jian L, Yu D, Shen W, Shen X and Chen Z 2012 *Appl. Phys. Lett.* **100** 101912
[20] Schmidt-Grund R, Rheinlaender B, Czekalla C, Benndorf G, Hochmut H, Rahm A, Lorenz M and Grandmann M 2007 *Superlattices & Microstruct.* **41** 360
[21] Kalusniak S, Sadofev S, Halm S and Henneberger F 2011 *Appl. Phys. Lett.* **98** 011101
[22] Halm S, Kalusniak S, Sadofev S, Wunsche H J and Henneberger F 2011 *Appl. Phys. Lett.* **99** 181121
[23] Deng H, Haug H and Yamamoto Y 2010 *Rev. Mod. Phys.* **82** 1489
[24] Timofeev V and Sanvitto D 2012 *Exciton Polaritons in Microcavities* (Berlin: Springer) Vol. 172
[25] Ferrier L, Wertz E, Johne R, Solnyshkov D D, Senellart P, Sagnes I, Lemaitre A, Malpuech G and Bloch J 2011 *Phys. Rev. Lett.* **106** 126401
[26] Bhattacharya P, Frost T, Deshpande S, Baten M Z, Hazari A and Das A 2014 *Phys. Rev. Lett.* **112** 236802
[27] Wertz E, Ferrier L, Solnyshkov D D, Johne R, Sanvitto D, Lemaître A, Sagnes I, Grousson R, Kavokin A V, Senellart P, Malpuech G and Bloch J 2010 *Nat. Phys.* **6** 860
[28] Su Y Q, Chen M M, Su L X, Zhu Y and Tang Z K 2016 *Chin. Phys. B* **25** 066106